Chemistry and Physics of Lipids 178 (2014) 52–62

Contents lists available at ScienceDirect

Chemistry and Physics of Lipids

journal homepage: www.elsevier.com/locate/chemphyslip

Influence of nanoparticle–membrane electrostatic interactions on membrane fluidity and bending elasticity

Poornima Budime Santhosh[a], Aljaž Velikonja[b,c], Šarka Perutkova[d,e], Ekaterina Gongadze[d], Mukta Kulkarni[d], Julia Genova[f], Kristina Eleršič[g], Aleš Iglič[d], Veronika Kralj-Iglič[h], Nataša Poklar Ulrih[a,i,*]

[a] Department of Food Science and Technology, Biotechnical Faculty, University of Ljubljana, Jamnikarjeva 101, SI-1000 Ljubljana, Slovenia
[b] Laboratory of Biocybernetics, Faculty of Electrical Engineering, University of Ljubljana, Tržaska 25, SI-1000 Ljubljana, Slovenia
[c] SMARTEH Research and Development of Electronic Controlling and Regulating Systems, Trg Tigrovcev 1, SI-5220 Tolmin, Slovenia
[d] Laboratory of Biophysics, Faculty of Electrical Engineering, University of Ljubljana, Tržaska 25, SI-1000 Ljubljana, Slovenia
[e] Institute of Cell Biology, Faculty of Medicine, University of Ljubljana, Lipičeva 2, SI-1000 Ljubljana, Slovenia
[f] Institute of Solid State Physics, Bulgarian Academy of Sciences, 1784 Sofia, Bulgaria
[g] Jožef Stefan Institute, Jamova 39, SI-1000 Ljubljana, Slovenia
[h] Laboratory of Clinical Biophysics, Faculty of Health Sciences, University of Ljubljana, Vrazov trg 2, SI-1000 Ljubljana, Slovenia
[i] Centre of Excellence for Integrated Approaches in Chemistry and Biology of Proteins (CipKeBiP), Jamova 39, SI-1000 Ljubljana, Slovenia

ARTICLE INFO

Article history:
Received 22 August 2013
Received in revised form
21 November 2013
Accepted 22 November 2013
Available online 2 December 2013

Keywords:
Nanoparticles
Liposomes
Membrane fluidity
Bending elasticity
Membrane electrostatics

ABSTRACT

The aim of this work is to investigate the effect of electrostatic interactions between the nanoparticles and the membrane lipids on altering the physical properties of the liposomal membrane such as fluidity and bending elasticity. For this purpose, we have used nanoparticles and lipids with different surface charges. Positively charged iron oxide (γ-Fe_2O_3) nanoparticles, neutral and negatively charged cobalt ferrite ($CoFe_2O_4$) nanoparticles were encapsulated in neutral lipid 1-stearoyl-2-oleoyl-sn-glycero-3-phosphocholine and negatively charged 1-palmitoyl-2-oleoyl-sn-glycero-3-phospho-L-serine lipid mixture. Membrane fluidity was assessed through the anisotropy measurements using the fluorescent probe 1,6-diphenyl-1,3,5-hexatriene. Though the interaction of both the types of nanoparticles reduced the membrane fluidity, the results were more pronounced in the negatively charged liposomes encapsulated with positively charged iron oxide nanoparticles due to strong electrostatic attractions. X-ray photoelectron spectroscopy results also confirmed the presence of significant quantity of positively charged iron oxide nanoparticles in negatively charged liposomes. Through thermally induced shape fluctuation measurements of the giant liposomes, a considerable reduction in the bending elasticity modulus was observed for cobalt ferrite nanoparticles. The experimental results were supported by the simulation studies using modified Langevin–Poisson–Boltzmann model.

1. Introduction

Liposomes with the potential to encapsulate the nanoparticles (NPs) find extensive applications in biomedical and pharmaceutical fields due to their ability to carry huge payload, improved stability, targeted delivery of the encapsulated material and to minimize the NPs toxicity (Torchilin, 2005; Uhumwangho and Okorr, 2005). For instance, liposomes encapsulated with ultrasmall superparamagnetic iron oxide NPs are gaining popularity in magnetic resonance imaging of cancer cells, diagnosis as well as treatment (Weinstein et al., 2010; Laurent and Mahmoudi, 2011). Since the NPs usage for *in vivo* applications are gradually increasing, it is crucial to investigate the various modes of NPs interaction with the bilayer lipids. Depending on the NPs concentration, their interaction with the bilayer lipids may alter the membrane properties and their functions (Albanese et al., 2012).

High density encapsulation of NPs in the liposomes is preferred in many clinical applications such as drug delivery and hyperthermia to achieve better results. Electrostatic interactions based on the surface charge of the liposomes and NPs plays an important role in determining the efficiency of NPs encapsulation in liposomes (Sipai Altaf Bhai et al., 2012). The surface charge of the liposomes can be altered by varying the lipid composition, pH and the external environment during liposome preparation. When charged lipids are used to prepare liposomes, they are more stable due to electrostatic repulsions which can prevent the aggregation and fusion of

* Corresponding author at: Department of Food Science and Technology, Biotechnical Faculty, University of Ljubljana, Jamnikarjeva 101, SI-1000 Ljubljana, Slovenia. Tel.: +386 13203780.
E-mail address: natasa.poklar@bf.uni-lj.si (N.P. Ulrih).

0009-3084/$ – see front matter © 2013 Elsevier Ireland Ltd. All rights reserved.
http://dx.doi.org/10.1016/j.chemphyslip.2013.11.009

neighbouring vesicles (Sybachin et al., 2012). Frokjaer et al. (1982) has demonstrated increased stability of phosphatidylcholine liposomes by decreasing the ionic strength and increasing the surface charge. The surface charge of the NPs can be modified by changing the functional groups attached to the NPs surface or by changing the coating material (Jiang et al., 2009). The NPs are coated with different materials such as polyethylene glycol, citric acid and dextran to increase their stability. The nature of the coating material greatly influences the zeta potential value of NPs. High zeta potential values of the NPs are a key factor to stabilize them in suspensions and to reduce their cytotoxicity (Wu et al., 2008).

To study the effect of surface charges and electrostatic interactions in detail, we have used a neutral lipid 1-stearoyl-2-oleoyl-sn-glycero-3-phosphocholine (SOPC) and its mixture with negatively charged 1-palmitoyl-2-oleoyl-sn-glycero-3-phospho-L-serine (POPS) to prepare the liposomes. Similarly we have used NPs with varying surface charges by adding different functional groups to their surface. Neutral and negatively charged $CoFe_2O_4$ NPs and positively charged γ-Fe_2O_3 NPs were encapsulated in both the type of liposomes. We have chosen magnetic NPs such as iron oxide and cobalt ferrite NPs for our work as they have vast expanding applications such as magnetofection, cell labeling, immunoassays and cancer therapy (Akbarzadeh et al., 2012). By the application of an external magnetic field, they can be easily manipulated to reach the target region for diagnosis, drug delivery and treatment (Santhosh and Ulrih, 2013).

The interaction of NPs with the phospholipid membrane affects the fluidity which can be studied through the anisotropy measurements using the fluorescent probes such as 1,6-diphenyl-1,3,5 hexatriene (DPH) (Hianik and Passechnik, 1995). Bilayer fluidity is related to the viscosity of the lipid membrane which is an important feature of the cell membrane. Increased fluidity enhances the free movement of phospholipid molecules and protein moieties in the membrane to facilitate various biological functions like ion transport, cell signaling and cell growth (Park et al., 2005). The fluidity of the bilayer/membrane can be affected by the membrane bound or encapsulated NPs (Roiter et al., 2008). Similarly the NPs adsorbed to the membrane surface or entrapped in the bilayer have a significant effect on the elastic properties of the membrane which is essential for the cell to perform the fundamental functions like adhesion, migration and interaction (Lai et al., 2013). Hence in order to better understand the influence of NPs in membranes, it is necessary to study the various effects of NPs interactions on cell membranes and model membranes.

Recent studies on the effects of NPs on membrane stability have revealed that the incorporation of metal NPs within the membrane alters the phase behavior of the lipids by decreasing the phase transition temperature and increasing the bilayer fluidity (Bhandary et al., 2011). Since the polymorphic phase behavior of lipids influence different membrane related processes, it has become important to study the effect of NPs interaction with different lipid membranes. Enormous research has been carried out with homogeneous bilayers consisting of zwitterionic phospholipids, but very less work has been done to understand the electrostatic attraction between the negatively charged lipid bilayers and differently charged NPs and its influence on the physical and chemical properties of membranes. Therefore the aim of our work is to study these interactions in detail through simulation studies and to establish a correlation between the theoretical calculations and the experimental results.

2. Materials and methods

SOPC and POPS lipids were purchased from Avanti Polar Lipids Inc., USA. DPH and HEPES [4-(2-Hydroxyethyl)piperazine-1-ethanesulfonic acid] were obtained from Sigma Aldrich Chemie GmbH, Steinheim, Germany. All the chemicals obtained have high purity (>99%) and used without any further purification. Negatively charged lipid vesicles were prepared by mixing SOPC and POPS lipids in the molar ratio of 4:1, respectively. Iron oxide and cobalt ferrite NPs were purchased from Nanotesla Institute, Ljubljana, Slovenia.

2.1. Synthesis of magnetic nanoparticles

Co-precipitation method was used to synthesize both the magnetic iron oxide and cobalt ferrite NPs. An aqueous mixture of ferric, ferrous salts and sodium hydroxide was prepared as an alkali stock solution (Wu et al., 2008; Mahnaz et al., 2013). The corresponding metal hydroxides were precipitated during the reaction between the alkaline precipitating reagent and the mixture of metal salts and subsequently oxidized in air to form γ-Fe_2O_3. The iron oxide NPs were coated with silica to ensure stability (Bumb et al., 2008) and attached with amino [NH_3^+] groups on their surface to impart positive charge. The dried iron oxide NPs were then dispersed in 20 mM HEPES buffer. The NPs were characterized using X-ray diffractometry and transmission electron microscopy (TEM) (see Fig. 2). The size of the synthesized γ-Fe_2O_3 NPs were found to be 10 ± 2 nm by TEM analysis and their zeta potential was found to be +40 mV using dynamic light scattering (DLS).

Aqueous $Fe(NO_3)_6 \cdot 9H_2O$ and $Co(NO_3)_2 \cdot 6H_2O$ solutions were mixed in stoichiometric ratios and served as precursors for the synthesis of cobalt ferrite NPs. To get the micelle solution, sodium dodecile sulfate was added and the resulting mixture was heated between 60 and 90 °C. To this mixture 10% NaOH solution was added to the mixture to set the pH between 9.5 and 11 and the synthesis temperature was maintained between 70 and 95 °C for about 4–5 h with continuous magnetic stirring. The mixture was centrifuged at a speed of 3000 rpm for 15 min. The supernatant was discarded and the remaining sample was centrifuged rapidly till a black precipitate was obtained. The precipitate was purified by washing thoroughly with water and acetone and dried in hot air oven at 100 °C for 2 h. The dried cobalt ferrite NPs were then dispersed in 20 mM HEPES buffer. To impart negative charge to their surface, the cobalt ferrite NPs were coated with citric acid. The size of the neutral and negatively charged cobalt ferrite NPs were found to be in the size range of 10–15 nm using TEM and their zeta potential values were found to be ± 34 mV and -40 mV for neutral and negatively charged cobalt ferrite NPs respectively using DLS instrument.

2.2. Preparation of nanoparticles encapsulated liposomes

Small unilamellar vesicles in the size range of 30–50 nm, encapsulated with iron oxide and cobalt ferrite NPs were prepared using thin film method. The lipids SOPC and SOPC–POPS mixture were dissolved in sufficient quantity of chloroform and then transferred into round bottomed flasks (Bangham et al., 1967). The organic solvent was evaporated completely under reduced pressure (1.7 kPa) using rotavapor to form a thin lipid film. The thin film was hydrated with a suspension of positively charged iron oxide, neutral and negatively charged cobalt ferrite NPs (1 mg/ml) suspended in 20 mM HEPES buffer at pH 7.0. The lipid suspension was then vortexed vigorously with glass beads for 10 min to prepare multilamellar vesicles (MLVs) and sonicated using a vibracell ultrasonic disintegrator VCX 750 (Sonics and Materials, Newtown, USA) with 50% amplitude and 10 s on-off cycles for 30 min to obtain small unilamellar vesicles (SUVs). The sample was then centrifuged at a speed of 14,000 rpm for 10 min to separate the debris formed after sonication (Eppendorf Centrifuge 5415C). The control SUVs were also prepared in a similar method but instead of NP suspension they were diluted with 1 mL of 20 mM HEPES buffer.

2.3. Anisotropy measurements

Anisotropy was measured using the incorporation of the fluorescent dye DPH (Li et al., 2013; Repakova et al., 2005) in the control liposomes and liposomes with encapsulated NPs using the Cary Eclipse fluorescence spectrophotometer (Varian, Mulgrave, Australia). The sample was transferred into a 10 mm-path-length cuvette. 10 μL of DPH (Sigma–Aldrich Chemie GmbH, Steinheim, Germany) in dimethyl sulphoxide (MerckKGaA, Darmstadt, Germany) was added to 2.5 mL 100 μM solutions of SUVs prepared from SOPC and SOPC–POPS mixture to reach a final concentration of 0.5 μM DPH. The anisotropy measurements were performed within the temperature range from 15 °C to 50 °C by gradually increasing the temperature 5 °C for every measurement with a time interval of 7 min with constant mixing at pH 7.0. Varian autopolarizers having slit widths with a nominal band-pass of 5 nm was used for both the excitation and emission spectra. The fluorescent probe DPH was excited at 358 nm with the excitation polarizer oriented in the vertical position. The emitted polarized light in both vertical and horizontal planes were recorded by a monochromator and measured at 410 nm. The anisotropy $\langle r \rangle$ values were measured using the built-in software of the instrument by applying the below formula:

$$\langle r \rangle = \frac{I_{\parallel} - GI_{\perp}}{I_{\parallel} + 2GI_{\perp}} \quad (1)$$

where, $I_{\parallel}$ and $I_{\perp}$ denotes the parallel and perpendicular fluorescence emission intensities. G is the correction factor for the scattered light and background fluorescence during fluorescence anisotropy measurements. The G-factor value for all the samples were determined individually by calculating the ratio of fluorescence intensities of vertically (I_{HV}) and horizontally polarized light (I_{HH}). From the anisotropy values, the lipid-order parameter S was calculated using the below formula (Pottel et al., 1983):

$$S = \frac{[1 - 2(r/r_0) + 5(r/r_0)^2]^{1/2} - 1 + r/r_0}{2(r/r_0)} \quad (2)$$

where r_0 denotes the fluorescence anisotropy measurements of DPH in the absence of any rotational motion of the probe. The theoretical value of r_0 of DPH is 0.4, and the experimental values of r_0 lie between the range of 0.362 and 0.394 (Pottel et al., 1983).

2.4. Preparation of giant unilamelar vesicles

The giant unilamellar liposomes were prepared with SOPC lipid through a modified electroformation technique (Angelova et al., 1992). 1 mg of the lipid was dissolved in 1 ml of chloroform and few drops of the resulting solution were placed on the surface of glass conductors coated with indium tin oxide (thickness of 100 ± 20 nm, sheet resistance of 100 Ω) which act as electrodes in the electroformation chamber. The glasses containing the lipid droplets were kept under high vaccum for 30 min to remove the chloroform completely. Once the dry lipid depots were formed, spacers were placed on the glass plates and filled with double distilled water. An alternative voltage of 1.5 V_{pp} and a low frequency of 10 Hz was applied to the conducting glass plates and kept overnight to form the giant vesicles.

2.5. Bending elasticity modulus

The analysis of thermally induced shape fluctuations of giant vesicles were used to study the influence of cobalt ferrite NPs on the bending elasticity of the membrane of giant neutral SOPC vesicles (Mitov et al., 1992). The giant vesicles were observed under a phase contrast microscope (Axiovert 100, Zeiss, Germany, oil immersion objective Ph3 100× magnification) to evaluate the fluctuations in the shape of the liposomes. The experimental equipment was improved by home-assembled stroboscopic illumination comprising an L6604 Xenon flash lamp, an E7289-01 external main discharge capacitor and a C6096 power supply, all from Hamamatsu, Japan. The images of the fluctuating GUVs were obtained with a C2400-60 camera (Hamamatsu, Japan) and the flash of the stroboscopic illumination was synchronized with the vertical pulses coming from the camera, with the light pulses lesser than 3–4 μs duration (full width at half maximum) at 2 J input energy. The data was recorded in the PC, analyzed with the AIS2 software (Genova and Mitov, 2013) and the bending elasticity modulus (k_c) values were measured by the thermal fluctuation method (Genova and Pavlic, 2012) as the weighted average value of about 7–8 vesicles. All of the experiments were performed in double distilled water environment.

2.6. X-ray photoelectron spectroscopy

The chemical composition of the control liposomes without NPs and liposomes encapsulated with the NPs were determined from the X-ray photoelectron spectroscopy (XPS) spectra. The samples were analyzed using the XPS instrument TFA XPS Physical Electronics. Since this analysis has to be carried out in high vacuum environment, a drop of the liposomes in buffer solution (10 μL) was placed onto a flat mica surface (110 Orientation) and dried completely. The dried sample was then placed in the XPS chamber and subsequently excited by the X-rays with a spot area over 400 μm^2 using a monochromatic Al $K_{\alpha 1,2}$ radiation at 1486.6 eV, with the pressure about 60 μPa. The photoelectrons were identified with a hemispherical analyzer which was positioned at an angle of 45° with respect to the normal to the sample surface. The spectral energy resolution was found to be about 0.6 eV. The individual elemental composition of the sample was measured from the spectra using the MultiPak v7.3.1 built-in software of the instrument.

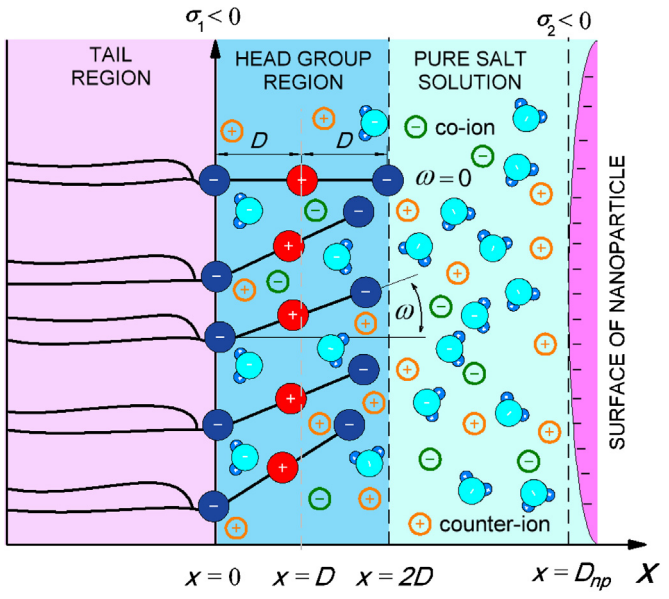

Fig. 1. Schematic presentation of the model to study the interaction between negatively charged POPS lipid and negatively charged NP suspended in salt solution. Negative charges at $x = 0$ are described as negative surface charge density σ_1. D is the distance between opposite charges within the head region, σ_2 is the surface charge density of charged NP, while ω describes the orientation angle of the single head group.

2.7. Analysis of encapsulation efficiency

The encapsulation efficiency (EE%) of NPs in the liposomes represents the percentage of NPs encapsulated into a liposome (Huang et al., 2005). The EE% value was calculated by measuring the ratio of the NPs concentration in the liposomes before and after the purification process. After sonication, the unbound $CoFe_2O_4$ and Fe_2O_3 NPs in the suspension were removed by centrifugation for 10 min at 12,000 $\times g$ to obtain pure SUVs encapsulated with NPs. The obtained SUVs were treated with methanol (1:10, v/v) and sonicated for 10 min to release the encapsulated NPs into the suspension. The concentration of the released NPs can be determined by using the UV-visible spectrophotometer at 300 nm. The encapsulation efficiency was determined using the following equation:

$$\text{Encapsulation efficiency}(\%) = \left[1 - \frac{\text{Amount of NPs in the encapsulated liposome}}{\text{Total amount of the NPs added during liposome preparation}}\right] \times 100. \quad (3)$$

2.8. Theoretical model

Contact of zwitterionic lipid layer with salt solution containing NPs was theoretically described using modified Langevin–Poisson–Boltzmann (MLPB) model (Velikonja and Perutkova, 2013; Gongadze et al., 2011a). MLPB model takes into account the cavity field in saturation regime, electronic polarization of water dipoles (Gongadze et al., 2011a,b; Gongadze and Iglič, 2012; Fröhlich, 1964) and the finite volumes of lipid head groups (Velikonja and Perutkova, 2013). The finite volume effect of other particles was not taken into account. The corresponding Poisson equation can be written as:

$$\frac{d}{dx}\left[\varepsilon_0\varepsilon_r(x)\frac{d\phi(x)}{dx}\right] = 2e_0n_0\sinh(e_0\phi(x)\beta) - \frac{e_0\mathcal{P}(x)}{Da_0} + \frac{e_0\mathcal{P}(x)}{2Da_0}, \quad (4)$$

where $\phi(x)$ is the electric potential, ε_0 is permittivity of vacuum, $\epsilon_r(x)$ is relative permittivity of salt solution, e_0 is elementary charge, n_0 is bulk concentration of salt, $\beta = 1/kT$, kT is the thermal energy, $\mathcal{P}(x)$ is the probability density function for angle ω (see Fig. 1), D is the distance between opposite charges in dipolar lipid head group and a_0 is the area per lipid molecule.

The boundary conditions are:

$$\frac{d\phi}{dx}(x = 0) = -\frac{\sigma_1}{\varepsilon_0\,\varepsilon_r(x = 0)}, \quad (5)$$

$$\frac{d\phi}{dx}(x = D_{np}) = \frac{\sigma_2}{\varepsilon_0\,\varepsilon_r(x = D_{np})}, \quad (6)$$

$$\phi(x = 2D_-) = \phi(x = 2D_+), \quad (7)$$

$$\frac{d\phi}{dx}(x = 2D_-) = \frac{d\phi}{dx}(x = 2D_+), \quad (8)$$

where in Eq. (5) the surface charge density at $x = 0$ is σ_1, while in Eq. (6) the surface charge density at $x = D_{np}$ is σ_2 corresponding to the surface charge density of NP (see also Fig. 1).

Eq. (4) was solved using standard implemented function for multi-boundary value problems (bvp4c) in Matlab2012b where the values $\epsilon_r(x)$ and $\mathcal{P}(x)$ were calculated in iteration process outside of bvp4c function. The $\varepsilon_r(x)$ within MLPB model is (Velikonja and Perutkova, 2013; Gongadze et al., 2011a):

$$\varepsilon_r(x) = n^2 + \frac{n_{0w}p_0}{\varepsilon_0}\left(\frac{2+n^2}{3}\right)\frac{\mathcal{L}(\gamma p_0 E(x)\beta)}{E(x)}, \quad (9)$$

where n is reffractive index of water, n_{0w} is concentration of water, p_0 is the dipole moment of water, $\mathcal{L}(u) = (coth(u) - 1/u)$ is Langevin function, $\gamma = (3/2)((2+n^2)/3)$ and $E(x) = |\phi(x)'|$ is the magnitude of the electric field, while the probability density function $\mathcal{P}(x)$ also takes into account the finite volumes of lipid headgroups and can be written as (Velikonja and Perutkova, 2013):

$$\mathcal{P}(x) = \Lambda\frac{\alpha\exp(-e_0\phi(x)\beta)}{\alpha(\exp(-e_0\phi(x)\beta) + 1)}, \quad (10)$$

where α is ratio between charged lipid head groups in the salt solution and all particles inside the head group region (see Fig. 1) and the value lambda (Λ) is calculated iteratively until the normalization condition is met (Fig. 2):

$$\frac{1}{D}\int_0^D \mathcal{P}(x)dx = 1. \quad (11)$$

3. Results and discussion

3.1. Bilayer fluidity

The influence of surface charge of the NPs and lipids ordering parameter and on bilayer fluidity of the liposomes was studied by the incorporation of fluorescent probe DPH into the liposomal bilayer and measuring the steady state fluorescent anisotropy values (Aricha et al., 2004; Kulkarni, 2012). The fluorescent probe DPH, as well as its derivatives are widely used to study the membrane properties such as polarity, fluidity and lipid ordering in the

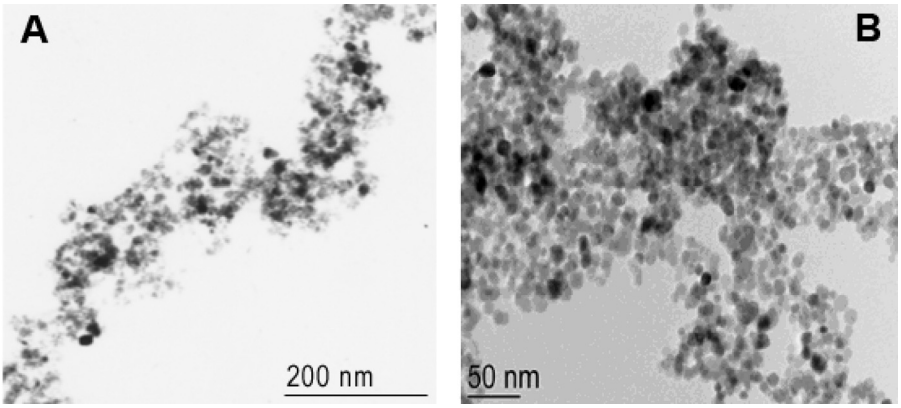

Fig. 2. TEM image of (A) neutral cobalt ferrite NPs and (B) iron oxide NPs.

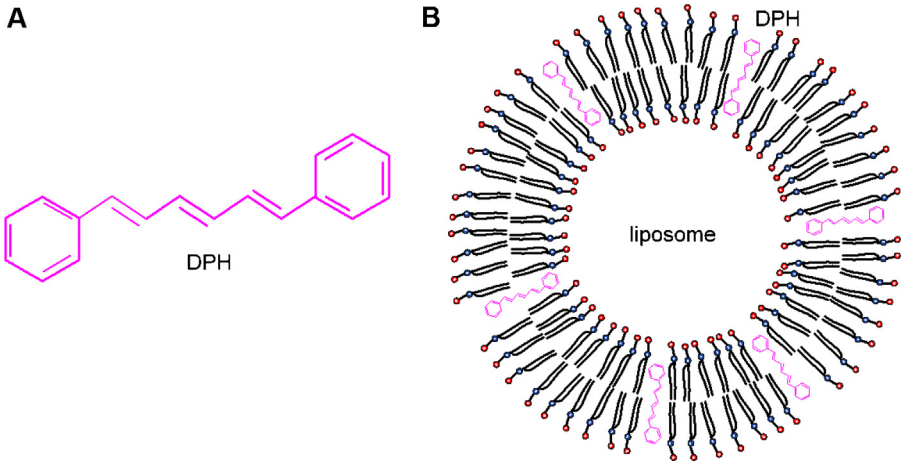

Fig. 3. (A) Structure of DPH molecule. (B) Schematic diagram illustrating the proposed incorporation of DPH in liposomes.

cell membranes as well as in liposomes (Perez-Berna et al., 2008; Spelios and Savva, 2008). The incorporation of DPH between the fatty acid tails in the bilayer is shown in Fig. 3. A notable feature of DPH is their ability to change their fluorescent properties depending on the environment. The dye is non-fluorescent in polar environment but after incorporating into the non-polar region of the bilayer, they emit strong fluorescence signals (Gmajner et al., 2011). They orient at various locations in the apolar tail region of the membrane and hence useful to study the entire organization and dynamics of the cell membranes as well as liposomes. The fluorescent anisotropy values of DPH correlate well with the rotational diffusion movement of the probe distributed throughout the bilayer and hence they are very sensitive in determining the packing order of the lipid chains and the membrane fluidity.

To study the effect of different NPs concentration and surface charge on the fluorescence anisotropy, positively charged Fe_2O_3 NPs, neutral and negatively charged $CoFe_2O_4$ NPs of varying concentrations such as 0.5, 1.0, 2.0, 3.0 and 5.0 mg were encapsulated in liposomes prepared with 1 mL of SOPC and SOPC–POPS lipids. The anisotropy values decreased gradually with decreasing NPs concentration in both the type of liposomes but the values decreased significantly in SOPC–POPS liposomes encapsulated with positively charged Fe_2O_3 NPs (data not shown). The result could be due to the strong electrostatic attractions between the oppositely charged surfaces leading to enhanced NPs encapsulation and the consequent disturbances in lipid ordering.

Anisotropy measurements are directly proportional to the ordering of membrane lipids and inversely proportional to the membrane fluidity; therefore reduced anisotropy values indicate increased membrane fluidity (Ulrih et al., 2009; Wrobel et al., 2012). The temperature changes induces the phase transition of the membrane lipids (Veksler and Gov, 2009). When the temperature increases, there is a transition from the rigid gel phase of the membrane lipids to the liquid phase. In such a phase, the mobility of the NPs in the membrane increases rapidly which disturbs the lipid ordering, induces the phase transition leading to decreased anisotropy values and increased membrane fluidity (Rappolt and Pabst, 2008).

The lipid-order parameter of neutral, positive and negatively charged NPs in the liposomes prepared with neutral lipid (SOPC) and negatively charged lipid (SOPC–POPS) mixture were shown in Fig. 4. The initial anisotropy and the corresponding order parameter values of DPH at 15 °C in case of SOPC liposomes were: 0.152 and 0.475 for control liposomes without NPs; 0.135 and 0.420 for neutral $CoFe_2O_4$ encapsulated liposome; and 0.116 and 0.357 for negatively charged $CoFe_2O_4$ encapsulated liposomes; and 0.150 and 0.468 for positively charged Fe_2O_3 incorporated liposomes. In SOPC–POPS mixtures the anisotropy values and corresponding order parameter values at 15 °C were: 0.136 and 0.423, 0.126 and 0.390, 0.135 and 0.420, 0.116 and 0.357 for control, neutral, negative and positively charged NPs loaded liposomes respectively. The standard error was ± 0.01 for all these measurements. In case of SOPC liposomes, the difference between the control and γ-Fe_2O_3 NPs was almost negligible due to the electrostatic repulsion

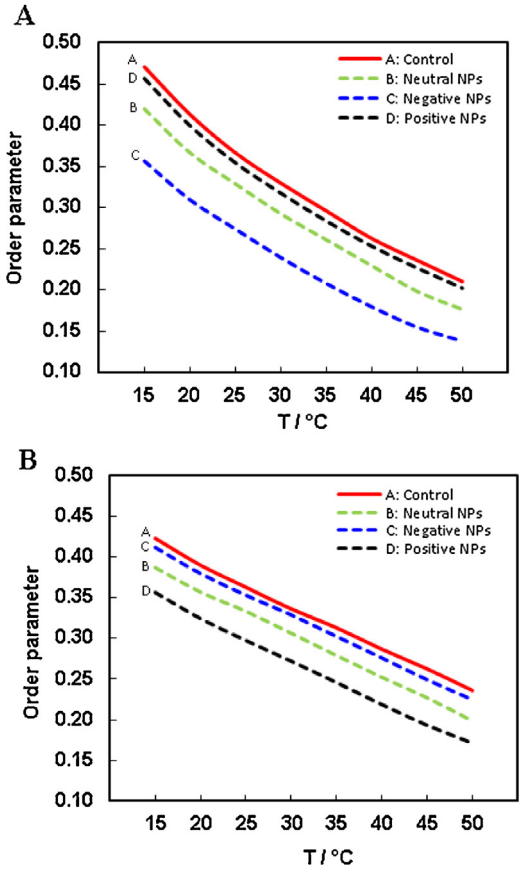

Fig. 4. Temperature dependent lipid-order parameter measurements of DPH following their incorporation into the liposomal membranes prepared from (A) SOPC, (B) SOPC–POPS lipid mixture. The liposomes were prepared at pH 7.0 and encapsulated with neutral and negatively charged cobalt ferrite NPs and positively charged iron oxide NPs.

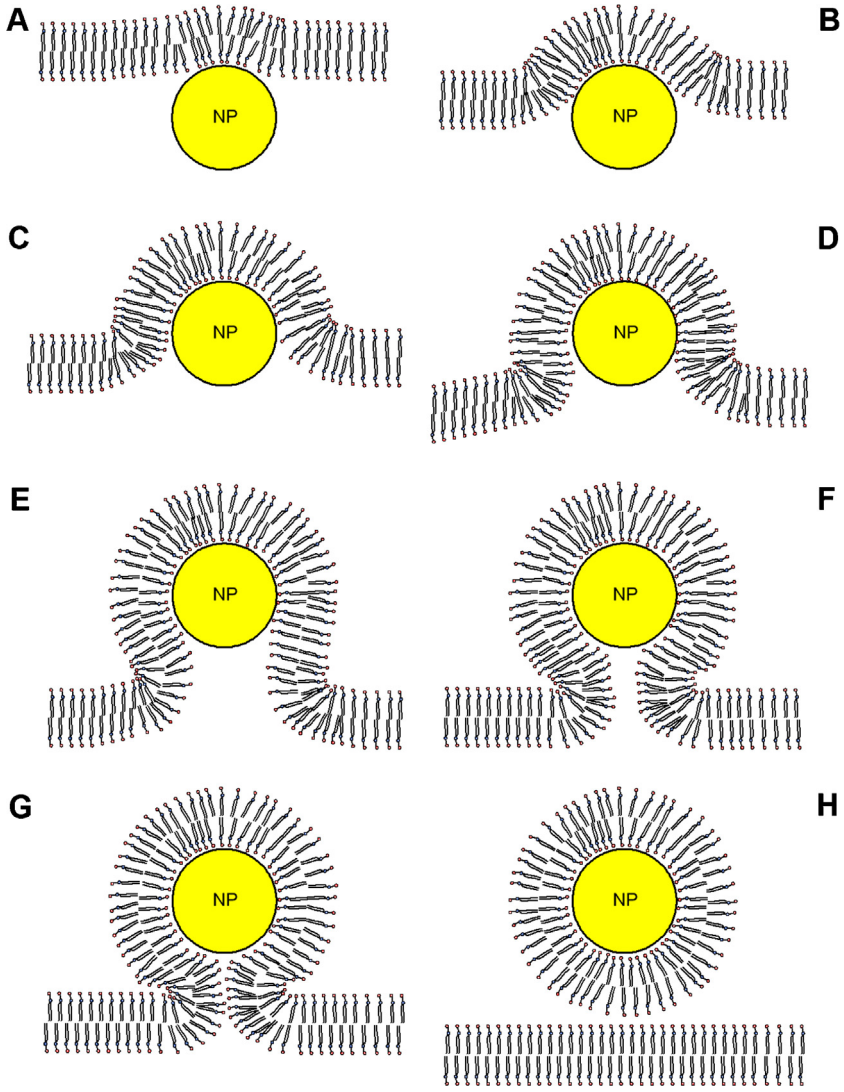

Fig. 5. Schematic figure showing the internalisation of larger NP inside the cell membrane. (A) NP adhesion to the membrane due to electrostatic attractive forces (B) initiation of membrane bending (C–E) membrane wrapping of the NP (F) neck formation (G) constriction of neck region (H) clevage of neck resulting in the internalisation of membrane encapsulated NP.

between the positively charged groups present in the lipid head and positively charged amino groups on the NP surface.

A similar effect was observed between the negatively charged SOPC–POPS mixture and negatively charged $CoFe_2O_4$ NPs. On the contrary, the difference was comparatively significant in the case of negatively charged SOPC–POPS and positively charged γ-Fe_2O_3 NPs. The attractive electrostatic forces between the cationic γ-Fe_2O_3 NPs and negatively charged SOPC–POPS lipid membrane enabled increased entrapment of NPs in the bilayer. These results indicate that electrostatic interactions play an important role in determining the efficiency of NPs encapsulation in liposomes as well as the interaction of NPs with the lipid membrane. If strong attractive electrostatic forces exists between the membrane and NPs surface, more amount of NPs will be encapsulated or adsorbed to the membrane leading to enhanced interactions (Michel and Gradzielski, 2012). This in turn will have a significant effect on the biophysical properties of the membrane. Some research groups have reported that even a small change in the fluorescence anisotropy values (up to 10%) caused a considerable change in the membrane viscosity (up to 25%) (Shinitzky and Barenholz, 1978). On the other hand, if electrostatic repulsions occur between the similarly charged liposome/membrane surface and the NPs, very less quantity of NPs will be encapsulated in the liposomes or enter into the cells. The obtained result is consistent with the findings of Bothun (2008) who demonstrated the encapsulation of silver NPs in liposomes decreased the anisotropy values and increased bilayer fluidity. Therefore our result coincides with the theoretical data, experimental results as well as with the simulations.

The adsorption of charged particles on the cell membrane due to strong electrostatic attractions leads to membrane deformation and alteration in the cell morphology (Hayden et al., 2012; Shlomovitz and Gov, 2009). Due to the negative surface charge of the cell membrane, NPs with the positive charge are attracted and internalised more compared to the neutral and negative NPs (Verma and Stellacci, 2010; Yaghmur and Rappolt, 2012). Though the size of the NPs exceed the width of the bilayer, due to membrane elasticity and flexibility the smaller NPs can be trapped partly or entirely into the bilayer. This entrapment of NPs disturbs the ordering of the lipids in the membrane leading to the changes in membrane fluidity. This result is supported by the fact that the cell membrane accommodates smaller intracellular proteins within itself and larger extracellular proteins partly embedded (encapsulated) in the lipid bilayer.

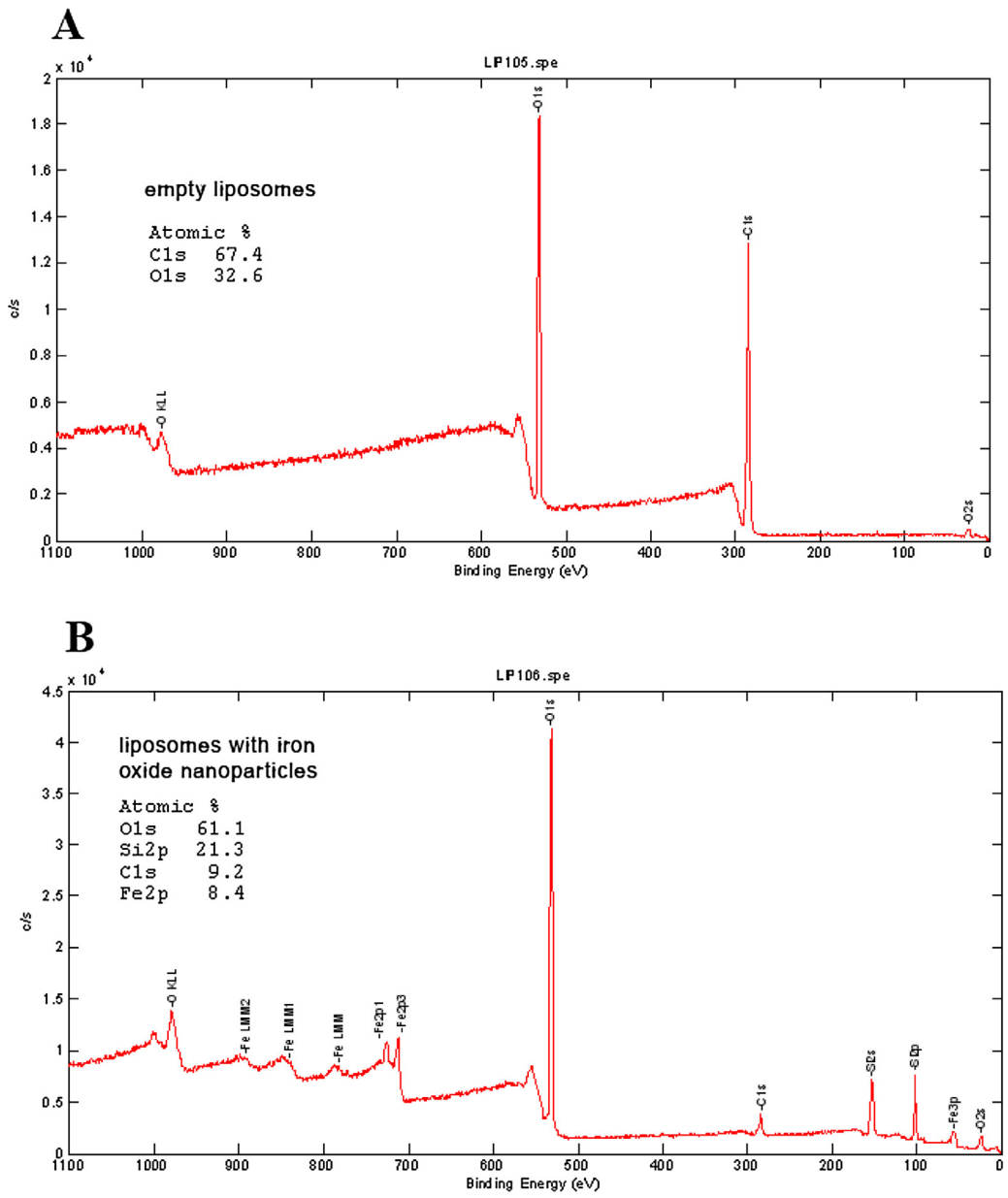

Fig. 6. XPS survey depicting the difference in chemical composition (at.%) between 2 spectrums. (A) Control liposomes without Fe_2O_3 NPs and (B) liposomes encapsulated with Fe_2O_3 NPs (Eleršič et al., 2012).

The cell membrane adopts different mechanisms for the NPs to pass through them and get internalised into the cell (Liu et al., 2009; Gladnikoff et al., 2009). A possible mode of encapsulation of a larger NP is shown in Fig. 5. Due to electrostatic attractive forces, the NPs approach and adhere to the membrane surface followed by membrane bending (Fig. 5(A and B)). If the adhesive forces between the NP and the membrane surface are strong enough to compensate the bending energy of the membrane, the membrane bends further forming a neck region to wrap the NP completely (Fig. 5(C–F)). Later the neck region constricts (Fig. 5G) further and cleave from the membrane due to thermal fluctuations, resulting in the formation of a bud in which the NP is entirely surrounded by the membrane and the encapsulated NP is subsequently released into the interior of the cell (Fig. 5H). Ruiz-Herrero et al. (2012) reported that the duration of membrane budding can be variable and the neck configurations during their observations lasted between 500 and 5000 τ_0.

3.2. XPS analysis

XPS is a widely used spectroscopic technique to analyze the surface chemistry of a sample using X-ray beams (Eleršič et al., 2012). The X-ray spectrum enables to determine the elemental composition, empirical formula and the electronic state of the individual elements in the sample. Since we anticipated that the positively charged NPs will be encapsulated more in the negatively charged liposomes due to strong electrostatic attractions, we used XPS to prove the NPs encapsulation in liposomes by determining the difference in the chemical composition between the control liposomes without NPs and SOPC–POPS liposomes encapsulated with the γ-Fe_2O_3 NPs.

The XPS spectra showing the difference between the empty liposomes and NPs encapsulated liposomes is shown in Fig. 6. The XPS spectra in the upper panel shows the chemical composition of the pure liposomes where one can observe the peaks depicting the presence of carbon and oxygen. The atomic composition of carbon

Table 1
Bending elasticity modulus (k_c) measurements of pure SOPC membrane and SOPC membrane with $CoFe_2O_4$ NPs.

System	Weighted mean value of the bending elasticity modulus $k_c/10^{-19}$ J	Number of vesicles
Pure SOPC membrane	2.1 ±0.1	8
SOPC membrane with $CoFe_2O_4$ NPs	1.6 ±0.1	7

Table 2
Encapsulation efficiency of neutral SOPC liposomes and negatively charged SOPC–POPS liposomes encapsulated with iron oxide and cobalt ferrite NPs ($n = 4$).

Sample	Encapsulation efficiency (%)
SOPC – Neutral $CoFe_2O_4$ NPs	79 ± 2.6
SOPC – Negative $CoFe_2O_4$ NPs	86 ± 1.7
SOPC – Positive Fe_2O_3 NPs	75 ± 4.2
SOPC–POPS – Neutral $CoFe_2O_4$ NPs	81 ± 2.2
SOPC–POPS – Negative $CoFe_2O_4$ NPs	65 ± 3.7
SOPC–POPS – Positive Fe_2O_3 NPs	94 ± 2.3

(C) in the prepared liposomes was found to be 67.4% whereas the oxygen (O) composition was 32.6%. The lower panel corresponds to the liposomes encapsulated with iron oxide NPs. Apart from the carbon and oxygen peaks, new peaks corresponding to iron (Fe) and silica (Si) were observed in the lower panel. By the appearance of Fe2p and Si2p signals in the XPS spectra, the presence of silica coated iron oxide NPs in the liposomes were confirmed. The chemical composition of the iron oxide NPs was also shown by the XPS results; higher concentration of oxygen (from 32.6 to 61.1 at.%) and the presence of Fe (8.4%) and Si (21.3%) were observed. The XPS measurement is very sensitive surface analysis method and the escape depth of photoelectrons is only a few nm. This is also the reason for higher concentration of silica which corresponds to the cover layer of iron oxide NPs.

3.3. Bending elasticity measurements

Bending elasticity is an important parameter that controls the membrane fluctuations or alterations in the shape of the vesicles mainly due to adhesion or interaction with different substances such as proteins, NPs or drugs. The analysis of thermally induced shape fluctuations of giant liposomes is a classical method for studying the elastic properties of lipid membranes. It is based on the fact that under the Brownian motions of water molecules, the lipid membrane in water environment constantly changes its shape due to the fluctuation. Such fluctuations of the biological or model membranes are a part of the phenomena, describing the deviation of some physical properties from their equilibrium state.

The obtained experimental data for the bending elasticity modulus (k_c) for pure SOPC membrane and for SOPC membrane with NPs are presented in Table 1. As it can be seen from the obtained results, the bending elasticity modulus decreases in the presence of neutral cobalt ferrite NPs in comparison with that of pure lipid membrane. This result is in good agreement with the theoretical predictions showing that lipid bilayers containing additives as different inclusions or attached molecules have at certain conditions reduced bending elastic modulus, which is mainly due to entropic effect (Kralj-Iglič et al., 1999; Bivas and Méléard, 2003; Iglič et al., 2007; Fošnarič et al., 2006; Meleard et al., 2011; Ramakrishnan et al., 2011).

3.4. Encapsulation efficiency

The lipid composition, surface charge of NPs, nature of the coating material and variation in the size of magnetic core of NPs are some of the important factors that influence the efficiency of NPs encapsulation in liposomes. Electrostatic interactions between the NPs surface and the liposomes are important to be considered to increase the NPs load in the vesicles. Our results (Table 2) showed the highest encapsulation efficiency of 94% between the negatively charged SOPC–POPS liposomes and positively charged Fe_2O_3 NPs due to strong electrostatic attractive forces between them. On the contrary, a lower EE% of 65% was obtained between the negatively charged SOPC–POPS liposomes and negatively charged $CoFe_2O_4$ NPs due to the electrostatic repulsions among the similar charges. To check the influence of varying NPs concentration on the encapsulation efficiency of liposomes, 0.5, 1.0, 2.0, 3.0 and 5.0 mg of NPs/mL of the lipid was used during the liposome preparation. In both the neutral and negatively charged liposomes, the EE% reached the highest for the vesicles with the lowest NPs concentration of 0.5 mg/mL such as of 89% and 93% respectively. The EE% gradually decreased with the increased NPs concentration in both the type of liposomes. This result is consistent with the findings of Sabate et al. (2008) and Frascione et al. (2012) who showed that EE% is inversely proportional to the initial NPs concentration. Increasing the NPs concentration above 3.0 mg/mL did not bring significant increase in EE%.

3.5. Theoretical discussion

POPS consists of two negative groups (phosphate and serine group) and one positive group (amino group) in the head region contributing a net negative surface charge to the lipid. Due to amphiphilic effect, the negative part of the head group bounded to lipid tails (phosphate group) is in contact with salt solution forming negatively charged surface. The positive part of lipid head group (amino group) and the outer negative part of the lipid head group (serine group) penetrates into the salt solution (see Fig. 1). The average orientation angle of the lipid head group $\langle\omega\rangle$ as a function of the distance of the NP (D_{np}) from the negatively charged part of lipid head groups at $x = 0$ can be seen in Fig. 7. The results were presented for three different values of parameter α and NPs with three

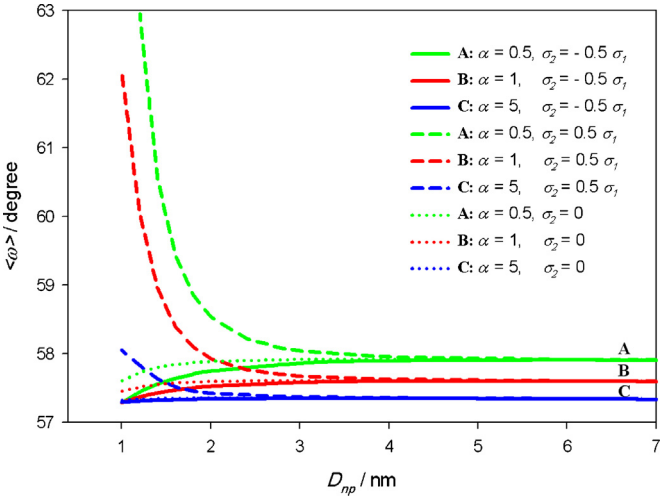

Fig. 7. The average orientation angle of the head group $\langle\omega\rangle$ as a function of the distance of NP (D_{np}) from negatively charged lipid surface at $x = 0$ for three different values of parameter α and NPs with three different charges: negative (solid plots), positive (dashed plots) and neutral (dotted plots). The values of used parameters were: $T = 298$ K, $\sigma_1 = -0.3$ As/m^2, dipole moment of water $p_0 = 3.1$ Debye, $D = 0.42$ nm, bulk concentration of salt $n_0/N_A = 0.1$ mol/L, concentration of water $n_{0w}/N_A = 55$ mol/L, where N_A is Avogadro number.

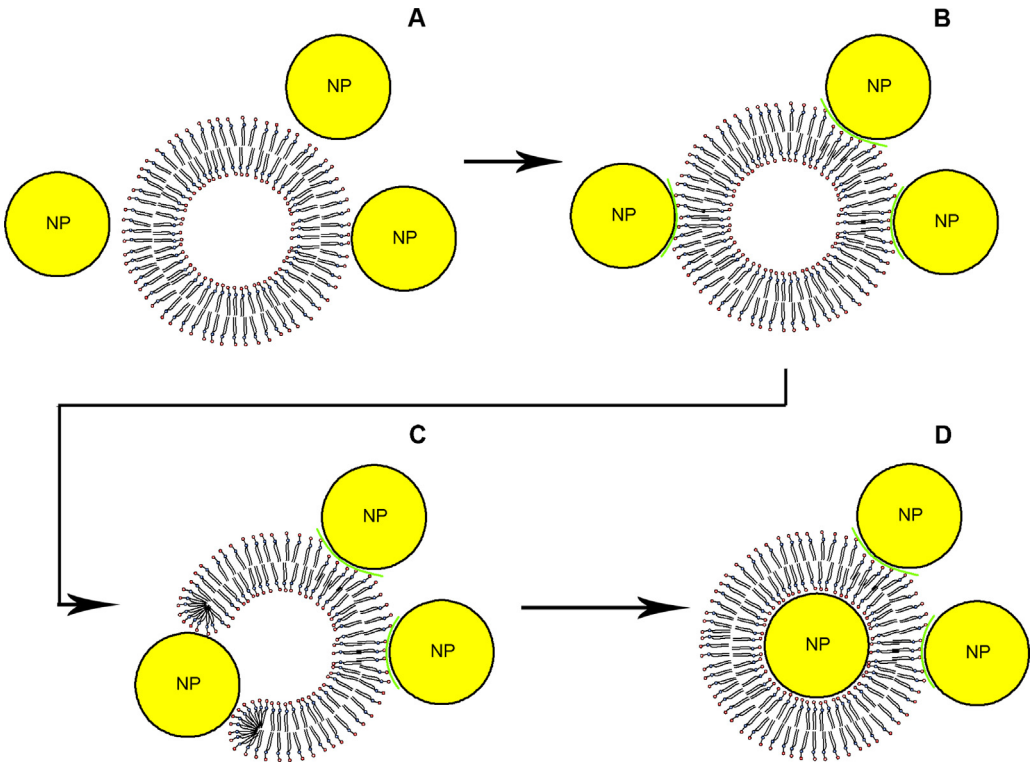

Fig. 8. Schematic diagram showing various possible modes of NPs interaction with the lipid membranes and their subsequent encapsulation. (A) approach of the charged NPs to the surface of the lipid membranes (B) attachment/adhesion of the NPs to the membrane surface and membrane bending (C) membrane pore formation by the NP (D) encapsulation of the NP in the core of the liposomes.

different charges (positive, neutral and negative). For negatively charged NP, it can be seen that with the decreasing distance D_{np} the average orientation angle of the lipid head group $\langle\omega\rangle$ increases significantly. For positively charged NP, weak attractive forces exist between the negatively charged part of lipid head group at $x = 2D$ and positively charged NP resulting in decreased average orientational angle $\langle\omega\rangle$ towards 57 degrees. For the neutral NP, the average orientation angle is practically constant.

3.6. Different possible modes of nanoparticle interaction with the membrane

Based on the results presented in Fig. 7 and the results of many previous studies we conclude that the surface charge of the lipid vesicles and NPs play an important role in determining the encapsulation ratio of the NPs in the liposomes (Arsov et al., 2009; Husen et al., 2012; Bernchou et al., 2011). Fig. 8A depicts the approach of NPs to the surface of the vesicles and in case of strong electrostatic attractions, the particles adsorb to the bilayer surface and may induce membrane bending as shown in Fig. 8B. A possible mode of NPs encapsulation inside the liposomes is through pore formation. Roiter et al. (2008) reported the formation of membrane pores by silica NPs in the size range of 1.2–22 nm in the phosphatidylcholine membranes. Fig. 8C depicts the NPs induced pore formation in membranes and Fig. 8D demonstrates their subsequent encapsulation in the aqueous core of the liposomes.

4. Conclusion

Small unilamellar vesicles encapsulated with neutral, negative and positively charged NPs were prepared with SOPC (neutral), SOPC-POPS lipid mixture (negatively charged) to study the influence of electrostatic interactions on fluidity and elasticity of liposomal membranes. The fluorescent anisotropy measurements showed a significant reduction in the fluidity of negatively charged SOPC-POPS liposomal membranes caused by the positively charged iron oxide NPs. The results from XPS spectra also confirmed that γ-Fe_2O_3 NPs were successfully encapsulated in the interior of the liposomes. The increased adhesion of positive NPs on the negatively charged liposomes was also suggested from theoretical MLPB model, where we predicted the stronger average orientation of lipid headgroups in direction perpendicular to the liposome membrane surface, corresponding to the attractive forces between the negatively charged serine groups of the POPS lipid and positively charged iron oxide NPs. The encapsulation of $CoFe_2O_4$ NPs in the SOPC membrane bilayer of giant unilamellar vesicles reduced the bending elasticity modulus of the lipid membrane. Our findings are consistent with our understanding that the electrostatic attractions between the membrane and NPs surface promote the encapsulation efficiency of NPs in liposomes and enhance their interactions with the membrane. These results will contribute to gain knowledge about the effect of magnetic NPs on the physical properties of the membrane and the significance of electrostatic forces in order to increase the NPs load in the vesicles which in turn is desirable for various clinical applications such as drug delivery and magnetic hyperthermia. Since the application of NPs in the biomedical field is tremendously increasing, our results describing the effect of magnetic NPs on physical properties of the membrane gains importance.

Conflicts of interest

The authors have no conflicts of interest to disclose in this work.

Acknowledgements

This work was in part supported by the Slovenian Research Agency (ARRS). P.B.S., E.G., and J.G. were mainly supported by the

grants from Slovenian Human Resources Development and Scholarship Fund, while A.V. by European social fund and SMARTEH. J.G. was also supported by the Internal Grant VK-02-13 of the Institute of Solid State Physics, Bulgarian Academy of Sciences.

References

Akbarzadeh, A., Samiei, M., Davaran, S., 2012. Magnetic nanoparticles: preparation, physical properties, and applications in biomedicine. Nanoscale Res. Lett. 7, 144.

Albanese, A., Tang, P.S., Chan, W.C.W., 2012. The effect of nanoparticle size, shape, and surface chemistry on biological systems. Annu. Rev. Biomed. Eng. 14, 1–16.

Angelova, M., Soléau, S., Méléard, P., Faucon, F., Bothorel, P., 1992. Preparation of giant vesicles by external AC electric fields. Kinetics and applications. In: Helm, C., Lösche, M., Möhwald, H. (Eds.), Trends in Colloid and Interface Science VI, Progress in Colloid and Polymer Science. Springer, Berlin/Heidelberg, Germany, pp. 127–131.

Aricha, B., Fishov, I., Cohen, Z., Sikron, N., Pesakhov, S., Khozin-Goldberg, I., Dagan, R., Porat, N., 2004. Differences in membrane fluidity and fatty acid composition between phenotypic variants of Streptococcus pneumoniae. J. Bacteriol. 186, 4638–4644.

Arsov, Z., Rappolt, M., Grdodolnik, J., 2009. Weakened hydrogen bonds in water confined between lipid bilayers: the existence of a long-range attractive hydration force. Chem. Phys. Chem. 10, 1438–1441.

Bangham, A., De Gier, J., Greville, G., 1967. Osmotic properties and water permeability of phospholipid liquid crystals. Chem. Phys. Lipids 1, 225–246.

Bumb, A., Brechbiel, M.W., Choyke, P.L., Fugger, L., Eggeman, A., Prabhakaran, D., Hutchinson, J., Dobson, P.J., 2008. Synthesis and characterization of ultra-small superparamagnetic iron oxide nanoparticles thinly coated with silica. Nanotechnology 19, 335601.

Bernchou, U., Midtiby, H., Ipsen, J.H., Simonsen, A.C., 2011. Correlation between the ripple phase and stripe domains in membranes. Biochim. Biophys. Acta 1808, 2849–2858.

Bhandary, S., Sultana, P., Basu, R., Das, S., Nandy, P., 2011. A study on modulation of phase behavior of lipid aggregates-effect of some metal NPs. Adv. Sci. Eng. Med. 3, 1–6.

Bivas, I., Méléard, P., 2003. Bending elasticity and bending fluctuations of lipid bilayer containing an additive. Phys. Rev. E 67, 012901.

Bothun, G.D., 2008. Hydrophobic silver NPs trapped in lipid bilayers: size distribution, bilayer phase behavior, and optical properties. J. Nanobiotechnol. 6, 13.

Eleršič, K., Pavlič, J., Iglič, A., Vesel, A., Mozetič, M., 2012. Electric-field controlled liposome formation with embedded superparamagnetic iron oxide NPs. Chem. Phys. Lipids 165, 120–124.

Fošnarič, M., Iglič, A., May, S., 2006. Influence of rigid inclusions on the bending elasticity of a lipid membrane. Phys. Rev. E 74, 051503.

Frokjaer, S., Hjorth, E.L., Worts, O., 1982. Stability and storage of liposomes. In: Bundgard, H., Hansen, A., Kofod, H. (Eds.), Optimization of Drug Delivery. Munkgaard, Copenhagen, p. 384.

Frascione, D., Diwoky, C., Almer, G., Opriessnig, P., Vonach, C., Gradauer, K., Leitinger, G., Mangge, H., Stollberger, R., Prassl, R., 2012. Ultrasmall superparamagnetic iron oxide (USPIO)-based liposomes as magnetic resonance imaging probes. Int. J. Nanomed. 7, 2349–2359.

Fröhlich, H., 1964. Theory of Dielectrics. Clarendon Press, Oxford, UK.

Genova, J., Mitov, M., 2013. Lectures: measuring bending elasticity of lipid bilayers. In: Iglič, A., Genova, J. (Eds.), Advances in Planar Lipid Bilayers and Liposomes. Elsevier, Amsterdam, pp. 1–27.

Gladnikoff, M., Shimoni, E., Gov, N.S., Rousso, I., 2009. Retroviral assembly and budding occur through an actin-driven mechanism. Biophys. J. 97, 2419–2428.

Gongadze, E., Iglič, A., 2012. Decrease of permittivity of an electrolyte solution near a charged surface due to saturation and excluded volume effects. Bioelectrochemistry 87, 199–203.

Gongadze, E., van Rienen, U., Kralj-Iglič, V., Iglič, A., 2011a. Langevin Poisson–Boltzmann equation: point-like ions and water dipoles near charged membrane surface. Gen. Physiol. Biophys. 30, 130–137.

Gongadze, E., van Rienen, U., Iglič, A., 2011b. Generalized Stern models of an electric double layer considering the spatial variation of permittivity and finite size of ions in saturation regime. Cell. Mol. Biol. Lett. 16, 549–576.

Genova, J., Pavlic, J.I., 2012. Realization of Marin Mitov idea for the stroboscopic illumination used in optical microscopy. Bulg. J. Phys. 39, 65–71.

Gmajner, D., Ota, A., Šentjurc, M., Ulrih, N.P., 2011. Stability of diether C25,25 liposomes from the hyperthermophilic archaeon Aeropyrum pernix K1. Chem. Phys. Lipids 164, 236–245.

Hayden, S.C., Zhao, G., Saha, K., Phillips, R.L., Li, X., Miranda, O.R., Rotello, V.M., El-Sayed, M.A., Schmidt-Krey, I., Bunz, U.H.F., 2012. Aggregation and interaction of cationic NPs on bacterial surfaces. J. Am. Chem. Soc. 134, 6920–6923.

Hianik, T., Passechnik, V.I., 1995. Bilayer Lipid Membranes: Structure and Mechanical Properties. Kluwer Academic Publishers, Dordrecht, Netherlands, pp. 138–157.

Huang, Y.Z., Gao, J.Q., Liang, W.Q., Nakagawa, S., 2005. Preparation and characterization of liposomes encapsulating chitosan nanoparticles. Biol. Pharm. Bull. 28, 387–390.

Husen, P., Fidorra, M., Haertel, S., Bagatolli, L., Ipsen, J.H., 2012. A method for analysis of lipid vesicle domain structure from confocal image data. Eur. Biophys. J. Biophys. 41, 161–175.

Iglič, A., Slivnik, T., Kralj-Iglič, V., 2007. Elastic properties of biological membranes influenced by attached proteins. J Biomech. 40, 2492–2500.

Jiang, J., Oberdorster, G., Biswas, P., 2009. Characterization of size, surface charge, and agglomeration state of nanoparticle dispersions for toxicological studies. J. Nanopart. Res. 11, 77–89.

Kralj-Iglič, V., Heinrich, V., Svetina, S., Žekš, B., 1999. Free energy of closed membrane with anisotropic inclusions. Eur. Phys. J. B 10, 5–8.

Kulkarni, C.V., 2012. Lipid crystallization: from self assembly to hierarchical and biological ordering. Nanoscale 4, 5779–5791.

Lai, K., Wang, B., Zhang, Y., Zheng, Y., 2013. Computer simulation study of nanoparticle interaction with a lipid membrane under mechanical stress. Phys. Chem. Chem. Phys. 15, 270–278.

Laurent, S., Mahmoudi, M., 2011. Superparamagnetic iron oxide nanoparticles: promises for diagnosis and treatment of cancer. Int. J. Mol. Epidemiol. Genet., 367–390.

Li, Q., Tang, G., Xue, S., He, X., Miao, P., Li, Y., Wang, J., Xiong, L., Wang, Y., Zhang, C., Yang, G.Y., 2013. Silica-coated superparamagnetic iron oxide nanoparticles targeting of EPCs in ischemic brain injury. Biomaterials 34, 4982–5499.

Liu, J., Sun, Y., Drubin, D.G., Oster, G.F., 2009. The mechanochemistry of endocytosis. PLoS Biol. 7, e1000204.

Mahnaz, M., Ahmad, M.B., Haron, M.J., Namvar, F., Behzad, N., Rahman, M.Z.A., Amin, J., 2013. Synthesis, surface modification and characterisation of biocompatible magnetic iron oxide nanoparticles for biomedical applications. Molecules 18, 7533–7548.

Meleard, P., Pott, T., Bouvrais, H., Ipsen, J.H., 2011. Advantages of statistical analysis of giant vesicle flickering for bending elasticity measurements. Eur. Phys. J. E Soft Matter 34, 1–14.

Michel, R., Gradzielski, M., 2012. Experimental aspects of colloidal interactions in mixed systems of liposome and inorganic nanoparticle and their applications. Int. J. Mol. Sci. 13, 11610–11642.

Mitov, M.D., Faucon, J.F., Méléard, P., Bothorel, P., 1992. Thermal fluctuations of membranes. In: Gokel, G.W. (Ed.), Adv. Supramol. Chem. JAI Press, Greenwich, pp. 93–139.

Park, S.H., Oh, S.G., Mun, J.Y., Han, S.S., 2005. Effects of silver NPs on the fluidity of bilayer in phospholipid liposome. Colloids Surf. B 44, 117–122.

Perez-Berna, A.J., Guillen, J., Moreno, M.R., Bernabeu, A., Pabst, G., Laggner, P., Villalain, J., 2008. Identification of the membrane-active regions of hepatitis C virus p7 protein: biophysical characterization of the loop region. J. Biol. Chem. 283, 8089–8101.

Pottel, H., van der Meer, W., Herreman, W., 1983. Correlation between the order parameter and the steady-state fluorescence anisotropy of 1,6-diphenyl-1,3,5-hexatriene and an evaluation of membrane fluidity. Biochim. Biophys. Acta 730, 181–186.

Ramakrishnan, N., Kumar, P.B.S., Ipsen, J.H., 2011. Modeling anisotropic elasticity of fluid membranes. Macromol. Theor. Simul. 20, 446–450.

Rappolt, M., Pabst, G., 2008. Flexibility and structure of fluid bilayer interfaces. In: Nag, K. (Ed.), Structure and Dynamics of Membranous Interfaces. John Wiley and Sons, Inc., Hoboken, NJ, USA, pp. 45–81.

Repakova, J., Holopainen, J.M., Morrow, M.R., McDonald, M.C., Capkova, P., Vattulainen, I., 2005. Influence of DPH on the structure and dynamics of a DPPC bilayer. Biophys. J. 88, 3398–3410.

Roiter, Y., Ornatska, M., Rammohan, A.R., Balakrishnan, J., Heine, D.R., Minko, S., 2008. Interaction of NPs with lipid membrane. Nano Lett. 8, 941–944.

Ruiz-Herrero, T., Velasco, E., Hagan, M.F., 2012. Mechanisms of budding of nanoscale particles through lipid bilayers. J. Phys. Chem. B 116, 9595–9603.

Sabate, R., Barnadas-Rodriguez, R., Callejas-Fernandez, J., Hidalgo-Alvarez, R., Estelrich, J., 2008. Preparation and characterization of extruded magnetoliposomes. Int. J. Pharm. 347, 156–162.

Santhosh, P.B., Ulrih, N.P., 2013. Multifunctional superparamagnetic iron oxide nanoparticles: Promising tools in cancer theranostics. Cancer Lett. 336, 8–17.

Shinitzky, M., Barenholz, Y., 1978. Fluidity parameters of lipid regions determined by fluorescence polarization. Biochim. Biophys. Acta 515, 367–394.

Shlomovitz, R., Gov, N.S., 2009. Membrane-mediated interactions drive the condensation and coalescence of FtsZ rings. Phys. Biol. 6, 046017.

Sipai Altaf Bhai, M., Vandana, Y., Mamatha, Y., Prasanth, V.V., 2012. Liposomes: an overview. J. Pharm. Sci. Innov. 1, 13–21.

Spelios, M., Savva, M., 2008. Novel N,N-diacyl-1,3-diaminopropyl-2-carbamoyl bivalent cationic lipids for gene delivery – synthesis, in vitro transfection activity, and physicochemical characterization. FEBS J. 275, 148–162.

Sybachin, A.V., Ballauff, M., Yaroslavov, A.A., 2012. Composition and properties of complexes between spherical polycationic brushes and anionic liposomes. Langmuir 28, 16108–16114.

Torchilin, V.P., 2005. Recent advances with liposomes as pharmaceutical carriers. Nat. Rev. Drug. Discov. 4, 145–160.

Uhumwangho, M.U., Okorr, R.S., 2005. Current trends in the production and biomedical applications of liposomes: a review. J. Biomed. Sci. 4, 9–21.

Ulrih, N.P., Gmajner, D., Raspor, P., 2009. Structural and physicochemical properties of polar lipids from thermophilic archaea. Appl. Microbiol. Biotechnol. 84, 249–260.

Veksler, A., Gov, N.S., 2009. Phase transitions of the coupled membrane-cytoskeleton modify cellular shape. Biophys. J. 93, 3798–3810.

Velikonja, A., Perutkova, š., Gongadze, E., Kramar, P., Polak, A., Maček-Lebar, A., Iglič, A., 2013. Monovalent ions and water dipoles in contact with dipolar zwitterionic lipid headroups—theory and MD simulations. Int. J. Mol. Sci. 14, 2846–2861.

Verma, A., Stellacci, F., 2010. Effect of surface properties on nanoparticle–cell interactions. Small 6, 12–21.
Weinstein, J.S., Varallyay, C.G., Dosa, E., Gahramanov, S., Hamilton, B., Rooney, W.D., Muldoon, L.L., Neuwelt, E.A., 2010. Superparamagnetic iron oxide nanoparticles: diagnostic magnetic resonance imaging and potential therapeutic applications in neurooncology and central nervous system inflammatory pathologies, a review. J. Cereb. Blood Flow Metab. 30, 15–35.
Wrobel, D., Kłys, A., Ionov, M., Vitovic, P., Waczulikowa, I., Hianik, T., Gomez-Ramirez, R., de la Mata, J., Klajnert, B., Bryszewska, M., 2012. Cationic carbosilane dendrimers-lipid membrane interactions. Chem. Phys. Lipids 165, 401–407.
Wu, W., He, Q., Jiang, C., 2008. Magnetic iron oxide nps: synthesis and surface functionalization strategies. Nanoscale Res. Lett. 3, 397–415.
Yaghmur, A., Rappolt, M., 2012. Structural characterization of lipidic systems under nonequilibrium conditions. Eur. Biophys. J. 41, 831–840.